

## Article

# Numerical Study on Elastic Parameter Identification of Large-Span Steel Truss Structures Based on Strain Test Data

Yuxin Zhang <sup>1,\*</sup>, Ao Zhou <sup>1</sup>, Helong Xu <sup>1</sup> and Hexin Zhang <sup>2</sup> <sup>1</sup> School of Civil Engineering, Shanghai Normal University, Shanghai 201400, China<sup>2</sup> School of Computing, Engineering and the Built Environment, Edinburgh Napier University, Edinburgh EH10 5DT, UK

\* Correspondence: zyx@shnu.edu.cn

**Abstract:** Large-span steel trusses are widely used in public buildings such as large-span factory buildings, exhibition halls, gymnasiums, and bridges because of their fast construction speed and easy industrial manufacturing. Due to construction errors and environmental factors, the material properties may change during their service life, and it is an important prerequisite for the structural safety assessment to identify the true material parameters of the structure. Among the many parameters, the elastic modulus is one that has the greatest impact on the accuracy of structural safety analysis. In this paper, a mathematical analysis model of elastic modulus identification was constructed, based on the strain test data and the improved gradient regularization method. The relationship between the strain test data and elastic moduli was established. A common finite element program based on the method was developed to identify the elastic modulus. A series of numerical simulations was carried out on a 53-element steel truss model to study the availability and numerical stability of the method. The effects of different initial values, numbers of strain tests, and locations of the strain test as well as the number of unknown parameters on the identification results were studied. The results showed that the proposed method had very high accuracy and computational efficiency. For the case of 53 unknown parameters without considering the test error, the identification accuracy could reach a  $1 \times 10^{-10}$  order of magnitude after only several iterations. This paper provides an effective solution to obtain the actual values of the elastic modulus of steel truss structures in practical engineering.

**Keywords:** parameter identification; regularization; gradient matrix; elastic modulus; strain

**Citation:** Zhang, Y.; Zhou, A.; Xu, H.; Zhang, H. Numerical Study on Elastic Parameter Identification of Large-Span Steel Truss Structures Based on Strain Test Data. *Buildings* **2022**, *12*, 1861. <https://doi.org/10.3390/buildings12111861>

Academic Editors: Zhiming Zhang, Mingming Song, Qipei (Gavin) Mei and Bo Yang

Received: 12 October 2022

Accepted: 2 November 2022

Published: 3 November 2022

**Publisher's Note:** MDPI stays neutral with regard to jurisdictional claims in published maps and institutional affiliations.



**Copyright:** © 2022 by the authors. Licensee MDPI, Basel, Switzerland. This article is an open access article distributed under the terms and conditions of the Creative Commons Attribution (CC BY) license (<https://creativecommons.org/licenses/by/4.0/>).

## 1. Introduction

Large-span steel truss structures are widely used in public buildings such as large-span factory buildings, exhibition halls, gymnasiums, and bridges because of their fast construction speed and easy industrial manufacturing [1,2]. Due to construction errors and environmental factors, the structural material properties may change during the service, and it is an important prerequisite for structural safety assessment to fully understand the real material parameters of the structure. Therefore, the parameter and damage identification of steel truss structures have been of significant concern.

Chang [3] presented the preliminary results of modal-parameter identification and vibration-based damage detection of a damaged steel truss bridge. Zhuo [4] studied the damage identification of bolt connections in steel truss structures by using sound signals. Luong [5] proposed a methodology to identify multiple axial forces in members of a truss structure based on the modal parameters. Luong [6] investigated the inverse identification of the stress state in axially loaded slender members of steel truss structures using measured dynamic data. Liu [7] adopted inverse sensitivity analysis to estimate the unknown system parameter perturbation from the difference between the observed output data and the corresponding analytical output data calculated from the original system model. Cho [8] performed system identification on the swing span of a steel truss bridge

dating from 1896 using acceleration data collected from a wireless sensor network (WSN). Terlaje [9] used displacement measurements resulting from applied static point loads as constraints in an optimization algorithm that employed optimality criterion methods to extract the cross-sectional properties of elements within a mathematical model of a structure. Chakraborty [10] presented a methodology to diagnose and quantify the damage at the element level in a truss structure with the measured static strain properties of the truss.

In the above works, we found that most of the parameter identification work for steel truss structures was based on the dynamic response test, and mainly identified the dynamic characteristics of the structure. Works based on the static test and identifying the elastic parameters of the structure are limited. This is mainly because the dynamic test method can achieve real-time monitoring without artificially applying loads and blocking traffic. However, because it is related to modal identification, there are higher requirements for the accuracy of the test instruments and identification methods. A disadvantage of the static test method is the need to apply a load to excite static response, which blocks traffic, but it has the advantage of a good identification effect and easy measurement of the required data. Moreover, the static equilibrium equation is only related to the nature of the structural stiffness, and it is easy to calculate the structural stiffness according to the measured static data. Additionally, the static test equipment is cheaper, the test technology is more advanced, and the deformation of the structure can be measured more accurately, so it is beneficial to study the elastic parameter identification method based on the static test. In fact, the damage detection method based on the static test has also received extensive attention in the field of civil engineering. Song [11] studied the problem of the optimal strain sensor placement in the damage detection of truss elements. Wang [12] identified moving train load parameters including the train speed, axle spacing, gross train weight, and axle weights based on the strain-monitoring data. Compared with other static response tests, the strain test has unique advantages because of the strain gauges' small mass, high accuracy, easy installation and fixation, and low comprehensive cost, so it is widely used in engineering [13–15].

The elastic modulus is also one of the most important parameters that affect the structural safety assessment because it directly affects the composition of the structural stiffness matrix. Although work on the elastic parameter identification of steel truss structures is limited, this problem has been widely considered in the field of mechanical inverse problems, and many research methods have been proposed. In these methods, the common approach is to reflect the local parameter variation onto the actual response value based on the relationship between the structural parameter variation and the actual measured data of a certain response. Then, the problem is transformed into the minimization of the objective function with the unknown parameters as the unknown variables and the minimum difference between the theoretical response value and the measured response value, which is also a typical engineering inverse problem. According to different solution methods, the problem can be subdivided into the neural network method [16,17], Levenberg–Marquardt method [18,19], Tikhonov regularization method [20–22], Gauss–Newton method [23], genetic algorithm [24], and so on.

The gradient regularization method (hereafter GRM) is a method for solving the inverse problem. It was first proposed in [25] and its applicability to one-dimensional hyperbolic equations (one-dimensional wave equations) was verified. The applicability of the GRM in identifying the parameters of two-dimensional elliptic operators was demonstrated in [26]. The nonlinear inverse problem is transformed into the problem of solving linear equations by expanding the unknown parameters in series with the supplementary conditions of the inverse problem. Then, the GRM is used to solve the ill-posed linear equations. This method starts from the generality of the inverse problem, without any special constraints, and is not limited by the space dimension when solving the inverse problem, so it is a very general method for solving the inverse problem. The GRM solves the difficulties of ill-posedness, strong nonlinearity, and large calculation requirement in the process of solving inverse problems, and its advantages of a high accuracy of calculation

results and short calculation time make it applicable in related fields. The elastic modulus of concrete dam was identified by using the GRM and the displacement monitoring data in Liu [27]. Zhang [28] realized the elastic modulus identification of bar structures based on the displacement test data and the GRM.

The choice of the regularization parameter  $\alpha$  during the solution process of the regularization method is very important. If  $\alpha$  is too large, the stability of the solution is guaranteed, but the accuracy is reduced; if  $\alpha$  is too small, the stability of the solution is difficult to guarantee. Based on the idea of homotopy mapping, Cui et al. [29] extended the solution path, effectively expanded the convergence domain, and reduced the dependence on the initial value of iteration. Reichel [30] et al. selected the appropriate regularization parameter when the truncated singular value decomposition method and LSQR iterative Krylov subspace could not accurately estimate the data error. Hua [31] et al. studied the selection of regularization parameters in model updates and proposed that the selection of adaptive regularization parameters was more effective than that of the fixed regularization parameters. Hansen [32] proposed a more efficient regularization parameter selection method based on the L curve. Bucataru et al. [33] studied the numerical reconstruction of thermal boundary data on a part of the boundary occupied by an anisotropic solid, and used gradient regularization to solve the inverse problem.

In this paper, the problem was transformed into identifying the elastic modulus of the structure by measuring the strain data at several points of the structure, which is a typical inverse problem of operator identification [34]. Based on the GRM, the diagonal elements of the Jacobi matrix in the solution process were normalized through linear transformation, which improved the solution speed and accuracy. A problem solution model was derived and constructed based on the strain test data and the improved gradient regularization–finite element method for the first time. A general finite element calculation program was developed. A series of numerical simulation tests were carried out on a 53-element steel truss model to study the availability and numerical stability of the method. The effects of different initial values, different numbers of strain test, different locations of the strain test, and the number of unknown parameters on the identification results were studied. The results showed that the proposed method had very high accuracy and computational efficiency. Without considering the test error, only a few iterations were needed, and the identification accuracy could reach the order of  $1 \times 10^{-10}$ . For large-scale calculation, the advantages of this work will be more prominent compared with the traditional optimal solution method, and the identification accuracy does not depend on the selection of the initial value, so it has strong practicability. The proposed method provides an effective solution for obtaining accurate design values of the elastic parameters of steel truss structures in practical engineering.

## 2. Elastic Parameter Identification Model Based on Strain Test Data

### 2.1. Mathematical Solution Model of the Problem

For any structural members, when we artificially add an external load,  $P$ , it will cause additional displacement and stress–strain changes, and the strain is actually a function of the displacement. The static equation of a steel truss structure solved by the structural finite element is:

$$[K(E)]\{U\} = \{P\} \quad (1)$$

$$\{\varepsilon\} = [B]\{U\} \quad (2)$$

where  $\{U\} = (u_1 \ u_2 \ \dots \ u_n)^T$  is a column vector composed of unknown node displacements and  $\{P\} = (q_1, q_2, \dots, q_n)^T$  is a column vector of known nodal loads;

$[K(E)] = \begin{pmatrix} k_{11}(E) & \dots & k_{1n}(E) \\ \vdots & \ddots & \vdots \\ k_{n1}(E) & \dots & k_{nn}(E) \end{pmatrix}$  is the global stiffness matrix of the structure; and  $E$  is the elastic modulus of the structure.

$B$  is the transfer matrix between the strain and displacement, which is determined according to the specific problem.

Formula (1) is the solution equation of the verse problem, that is, to solve the response with the given load action and design parameter information. The correlation between the elastic modulus and strain,  $\varepsilon$ , is established by Equation (1). However, if the design parameters are unknown and the load and test data of the local response are known, can the information of design parameters be obtained by reverse solving? This is a typical inverse problem of operator identification. If the structure is regarded as a continuum in a certain spatial domain, and  $E$ ,  $\varepsilon$ , and  $P$  are functions about  $x$ , then the following mathematical equations for solving the inverse problem can be established:

$$K(E(x))U(x) = P(x) \quad x \in \partial R^r \quad (3)$$

$$\varepsilon(x) = [B(x)]U(x) \quad (4)$$

$$B_1(\varepsilon(x)) = \varepsilon_c(x) \quad x \in \partial R1^r \quad (5)$$

$$B_2(\varepsilon(x))_{x=x_s} = \varepsilon_s(x) \quad x \in \partial R2^r \quad (6)$$

where  $K$  is the operator of  $E(x)$ ;  $B_1, B_2$  is the boundary condition operator and the additional condition operator, respectively;  $s = 1, m$ , and  $m$  is the number of known strain test data.  $R$  is the spatial domain of the problem, equal to 2 or 3 for the plane and spatial domain problems, respectively;  $x$  is the coordinate defined on  $R^r$ ;  $R_1^r$  is the domain of given boundary conditions;  $R_2^r$  is the domain of the given supplementary conditions.

## 2.2. Establishing the Objective Function

Since only the strain data at the positions of the representative elements can be obtained, the solution of the problem described in Equations (3)–(6) is not unique, and only a set of optimal solutions satisfying the additional strain test data can be found. Considering the existence of the test error and numerical error, this paper used the strain relative value to establish the following constraint objective function.

Seeking  $E$ :

$$\text{Let } f(E) \leq \text{err} \quad (7)$$

$$f(E) = \sum_{i=1}^s |\tilde{\varepsilon}_i(E)| \quad (8)$$

$$\tilde{\varepsilon}_i(E) = \frac{\varepsilon_{si} - \varepsilon_i}{\varepsilon_{si}} \quad (9)$$

where  $\text{err}$  is a very small given value;  $\varepsilon_{si}$  is strain test data for the  $i$ th element;  $\varepsilon_i$  is the calculated strain value for the  $i$ th element.

## 2.3. Solution of Gradient Regularization Method [25] Based on Strain Test Data

Assuming the strain test data,  $\varepsilon^*(x)$ , is an exact solution satisfying Equations (3)–(6),  $\varepsilon^*(x)$  and the supplementary condition  $B_2(\varepsilon^*(x))$  are expanded by first-order Taylor expansion in the vicinity of  $E_0(x)$ , then there will be:

$$\varepsilon^*(x) = \varepsilon_0(x) + \int_R \frac{\partial \varepsilon(x)}{\partial E(x')} \Delta E(x') dx' \quad (10)$$

$$B_2(\varepsilon^*(x)) = B_2(\varepsilon_0(x)) + \int_R \frac{\partial B_2(\varepsilon(x))}{\partial E(x')} \Delta E(x') dx' \quad (11)$$

Since  $\varepsilon^*(x)$  is an exact solution, we have

$$B_2(\varepsilon^*(x)) = \varepsilon_s(x) \quad (12)$$

If we make:

$$D(x) = \varepsilon_s(x) - B_2(\varepsilon_0(x)) \quad (13)$$

$$G(E(x'), x) = \frac{\partial B_2(\varepsilon(x))}{\partial E(x')} \quad (14)$$

then we substitute Equations (12)–(14) into Equation (11) to obtain:

$$\int_R G(E(x'), x) \cdot \Delta E(x') dx' = D(x) \quad (15)$$

Here,  $G(E(x'), x)$  is the gradient operator of the supplementary condition  $\partial B_2(\varepsilon(x))$  to  $E(x')$  at  $E(x') = E_0(x')$ .

This is an ill-posed problem, hence, we construct the regularization functional:

$$J(\Delta E(x), \alpha) = \rho^2 \left( \int_W G(k(x'), x) \Delta E(x') dx', D(x) \right) + \alpha \Theta(\Delta E(x')) \quad x' \in W, x \in \partial W_2 \quad (16)$$

$$\rho^2 \left( \int_W G(E(x'), x) \Delta E(x') dx', D(x) \right) = \int_{\partial W_2} \left( \int_W G(E(x'), x) \Delta E(x') dx' - D(x) \right)^2 dx \quad (17)$$

Find  $\Delta E(x')$  from Formula (18):

$$\min J(\Delta E(x'), \alpha) = \rho^2 \left( \int_R G(E(x'), x) \Delta E(x') dx', D(x) \right) + \alpha \Theta(\Delta E(x')) \quad (18)$$

where  $\alpha$  is the regularization parameter and  $\Theta(\Delta E(x'))$  is the regularization functional. Equation (18) is discretized to give:

$$\min J(\Delta \tilde{E}, \alpha) = (\tilde{G} \cdot \Delta \tilde{E} - \tilde{D})^T (\tilde{G} \Delta \tilde{E} - \tilde{D}) + \alpha (\tilde{D} \Delta \tilde{E})^T (\tilde{R} \Delta \tilde{E}) \quad (19)$$

Let the first-order partial derivative of Equation (19) be equal to 0, and the extreme value of Equation (19) can be obtained as follows:

$$(\tilde{G}^T \tilde{G} + \alpha \tilde{H}) \Delta \tilde{E} = \tilde{G}^T \tilde{D} \quad (20)$$

where  $\tilde{H}$  is the derived matrix of  $\Theta(E(x'))$ .

For a linear problem,  $\Delta \tilde{E}$  can be solved from Equation (20). For a nonlinear problem, it needs to be solved by many iterations, thus:

$$\tilde{E}_{n+1} = \tilde{E}_n + \Delta \tilde{E}_n \quad (21)$$

When the convergence condition of Equation (21) is satisfied, the value  $E_{n+1}$  is taken as the real elastic modulus.

### 3. Improvement of Gradient Regularization Method [28]

The regularization parameter,  $\alpha$ , plays a key role in the process of solving the inverse problem, and it will affect the stability and accuracy of the solution. When it becomes large, the stability of the solution is improved, but the accuracy is reduced, and vice versa when it becomes small. Therefore, the choice of  $\alpha$  is key to the balance between the accuracy and stability.

In the original GRM, when looking for the parameters, the values are completely different in each iteration, even by several orders of magnitude. The search for  $\alpha$  is difficult. Therefore, based on the original GRM, the following linear transformation was adopted to normalize the diagonal elements of the Jacobi matrix.

After discretization, we have:

$$G = (G_1 \dots G_j \dots G_n) \quad (22)$$

$$\Delta E = (\Delta E_1 \dots \Delta E_j \dots \Delta E_n)^T \quad (23)$$

$$G_j = (G_{1j} \dots G_{ij} \dots G_{mj})^T = \left( \frac{\partial B_1}{\partial E_j} \dots \frac{\partial B_i}{\partial E_j} \dots \frac{\partial B_m}{\partial E_j} \right)^T \quad (24)$$

where  $n$  is the number of unknown elastic moduli and  $m$  is the number of supplementary test data. Let:

$$\bar{G} = \left( \frac{G_1}{\|G_1\|_2} \dots \frac{G_j}{\|G_j\|_2} \dots \frac{G_n}{\|G_n\|_2} \right) \quad (25)$$

$$\Delta \bar{E} = (\|G_1\|_2 \Delta E_1 \dots \|G_j\|_2 \Delta E_j \dots \|G_n\|_2 \Delta E_n)^T \quad (26)$$

Equation (15) is discretized as:

$$\tilde{G} \Delta \tilde{E} = \tilde{D} \quad (27)$$

Substituting  $\bar{G}$ ,  $\Delta \bar{E}$  into Equation (20):

$$\left( \bar{G}^T \bar{G} + \alpha \tilde{R}^T \tilde{R} \right) \Delta \bar{E} = \bar{G}^T \tilde{D} \quad (28)$$

where

$$\bar{G}^T \bar{G} = \left( \frac{G_i^T}{\|G_i\|_2} \cdot \frac{G_j}{\|G_j\|_2} \right)_{n \times n} \quad (29)$$

When  $i = j$ ,

$$\frac{G_i^T}{\|G_i\|_2} \cdot \frac{G_j}{\|G_j\|_2} = \frac{G_i^T}{\|G_i\|_2} \cdot \frac{G_i}{\|G_i\|_2} = 1 \quad (30)$$

$$\Delta \tilde{E} = \left\{ \frac{\Delta \tilde{E}_1}{\|G_1\|_2} \dots \frac{\Delta \tilde{E}_j}{\|G_j\|_2} \dots \frac{\Delta \tilde{E}_n}{\|G_n\|_2} \right\}^T \quad (31)$$

So far, the Jacobi matrix is normalized, which will not only improve the search speed, but also increase the accuracy of its solution.

#### 4. Numerical Experiments and Analysis

To verify the method in this paper, a typical steel truss bridge model was selected, and a series of numerical experiments were carried out with the common finite element analysis program developed with Fortran Language based on the GRM method.

##### 4.1. Prototype for Numerical Experiments

As shown in Figure 1, a plane steel truss model was selected for the numerical simulation analysis [35]. In this structure, each bar had a pipe cross section with an outer diameter of 1.71 cm, and a wall thickness of 0.2 cm. The total length of the truss was 5.6 m, with 0.4 m in each bay, and the height of the truss was 0.4 m. The model has 53 bar elements, 28 nodes, and 81 degrees of freedom. Among them, Nos. 1–14 elements were lower chord bars; No. 15–26 elements were upper chord bars; Nos. 27–53 elements were vertical bars, and the material parameters of each bar was the same (see Table 1 for specific parameter information). The bars were connected at pinned joints. There were two supports in this truss structure: a pin support at the left end and a roller support at the right end of the lower chord. The roller support at the right end was constrained in the vertical direction.

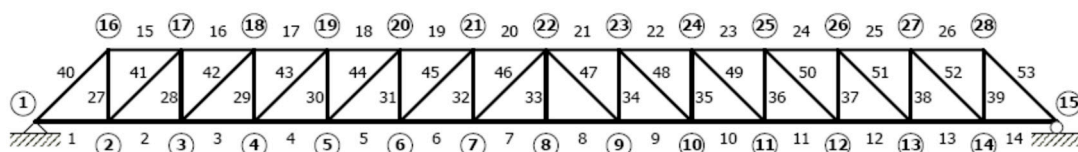


Figure 1. Schematic diagram of the plane hinged truss model.

**Table 1.** Basic material parameters of the truss bridge.

Parameter	Value
Modulus of elasticity, E	$2.0 \times 10^8$ Pa
Moment of inertia, I	$3.556 \times 10^{-4}$ m <sup>4</sup>
Section area of each bar, A	$1.38 \times 10^{-4}$ m <sup>2</sup>
Density, $r$	$5.69 \times 10^7$ kg/m <sup>3</sup>

It was assumed that the external load acts on node 21,  $F = -10$  kN (vertically downward), and the strain value of each element can be calculated through the verse problem calculation with the known design values of material parameters, as shown in Table 2.

**Table 2.** The calculated strain value of each element.

Element	Strain ( $\times 10^{-3}$ )	Element	Strain ( $\times 10^{-3}$ )
1	9.54	28	8.13
2	9.17	29	7.23
3	8.46	30	5.96
4	7.40	31	4.34
5	5.98	32	2.35
6	4.25	33	3.54
7	2.45	34	2.35
8	2.45	35	4.34
9	4.25	36	5.96
10	5.98	37	7.23
11	7.40	38	8.13
12	8.46	39	8.67
13	9.17	40	9.11
14	9.54	41	8.74
15	9.17	42	8.02
16	8.45	43	6.94
17	7.38	44	5.49
18	5.96	45	3.69
19	4.21	46	1.53
20	2.21	47	1.53
21	2.21	48	3.69
22	4.21	49	5.49
23	5.96	50	6.94
24	7.38	51	8.02
25	8.45	52	8.74
26	9.17	53	9.11
27	8.67		

#### 4.2. Study on the Availability of the Method

To verify the availability of the method, it was assumed that the material parameters are unknown. To simplify the problem of the regularity study of the method, the initial elastic modulus values of the bottom chord, the middle web member, and top chord were assumed to be the same and set as E1, E2 and E3, respectively, according to the position of the member; these values were estimated according to experience. The strain values of elements 2, 21, 36, and 44 were obtained by the verse problem calculation as the simulated strain test data. The termination criterion was set to  $1 \times 10^{-10}$ . If the method is correct, the design parameter values will be identified. The iteration process of the numerical experiment is shown in Table 3.

**Table 3.** Iteration process (unit:  $10^8$  N/m<sup>2</sup>).

Step	E1	E2	E3	Objective Function
E0	1.00	1.50	1.80	/
1	1.49	1.85	2.02	$7.55 \times 10^{-1}$
2	1.87	1.97	2.00	$1.51 \times 10^{-1}$
3	1.99	2.00	2.00	$9.01 \times 10^{-3}$
4	2.00	2.00	2.00	$2.68 \times 10^{-5}$
5	2.00	2.00	2.00	$6.68 \times 10^{-9}$
6	2.00	2.00	2.00	$2.16 \times 10^{-13}$
True value	2.00	2.00	2.00	

The data in Table 3 show that the calculated elastic modulus value finally converged to the design value of the model and satisfied the requirement of the objective function in the sixth iteration step, which proves the availability of the method and reflects its high efficiency.

#### 4.3. Elastic Parameter Identification under Different Initial Elastic Moduli Values

The strains of elements 2, 21, 36, and 44 were still selected as supplementary conditions for the inversion calculation. Three groups of different elastic moduli values were taken as the initial elastic moduli values, and the calculation results are shown in Table 4 (the iteration convergence progress is shown in Figure 2). The identification results in Table 4 show that the selection of the initial value of the elastic moduli had little effect on the identification results as long as the supplementary test information was accurate, but it would have a certain impact on the identification speed. However, because of the high efficiency of the GRM, the impact on the computational efficiency was almost negligible. Still, for large-scale engineering calculations in practical application, the initial value should be estimated according to the engineering information as far as possible to improve the calculation efficiency as much as possible. The information can be the initial design value of the elastic modulus in the design files, or some test data at the beginning of construction, etc.

#### 4.4. Effect of Amounts of Strain Test Data on the Identification Results

The initial elastic moduli values  $(1.3, 1.6, 1.9) \times 10^8$  N/m<sup>2</sup> were selected, along with different amounts of strain data from Table 2 as supplementary conditions to conduct the numerical simulation. The calculation results are shown in Table 5 (the convergence process is shown in Figure 3).

**Table 4.** Iteration results with different initial values.

Set No.	Initial Value ( $\times 10^8$ N/m <sup>2</sup> )	Total Iteration Steps	Solution ( $\times 10^8$ N/m <sup>2</sup> )	Error (%)
1	E1 = 1.0	6	2.0	$2.10 \times 10^{-11}$
	E2 = 1.3		2.0	$5.80 \times 10^{-11}$
	E2 = 1.5		2.0	$7.85 \times 10^{-11}$
2	E1 = 1.2	5	2.0	$7.65 \times 10^{-10}$
	E2 = 1.5		2.0	$6.20 \times 10^{-10}$
	E3 = 1.7		2.0	$5.60 \times 10^{-11}$
3	E1 = 1.3	5	2.0	$5.14 \times 10^{-10}$
	E2 = 1.6		2.0	$2.86 \times 10^{-10}$
	E3 = 1.9		2.0	$3.00 \times 10^{-12}$

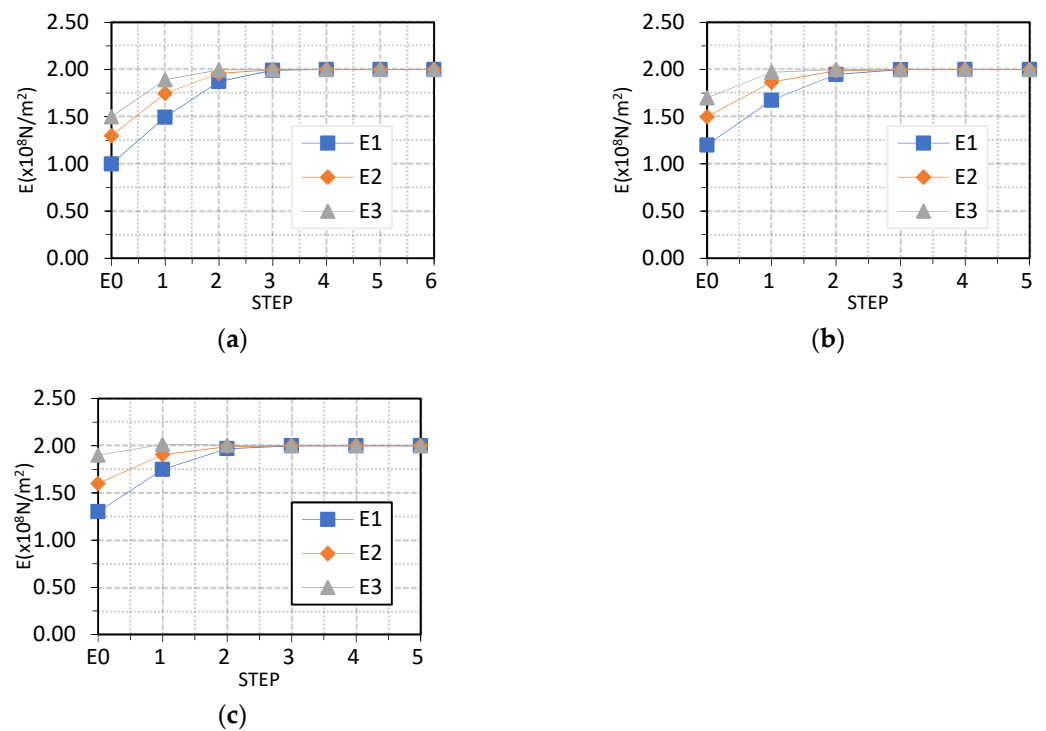


**Figure 2.** Results under different sets of initial values. (a) Results under the first set of initial values. (b) Results under the second set of initial values. (c) Result under the third set of initial values.

**Table 5.** Results with different numbers of strain test data ( $\times 10^8 \text{ N/m}^2$ ).

Number of Strain Test Data	Total Iteration Steps	E1, E2, E3	Error (%)
2	5	1.69	−15.5%
		1.71	−14.5%
		3.57	157.0%
3	5	2.0	$4.77 \times 10^{-10}$
		2.0	$1.74 \times 10^{-10}$
		2.0	$1.00 \times 10^{-11}$
5	5	2.0	$5.43 \times 10^{-10}$
		2.0	$1.38 \times 10^{-10}$
		2.0	$2.50 \times 10^{-12}$
10	5	2.0	$8.61 \times 10^{-10}$
		2.0	$9.85 \times 10^{-11}$
		2.0	$1.15 \times 10^{-11}$
15	5	2.0	$9.72 \times 10^{-10}$
		2.0	$2.10 \times 10^{-10}$
		2.0	$5.00 \times 10^{-13}$
53	6	2.0	$1.15 \times 10^{-11}$
		2.0	$1.20 \times 10^{-11}$
		2.0	$1.10 \times 10^{-11}$

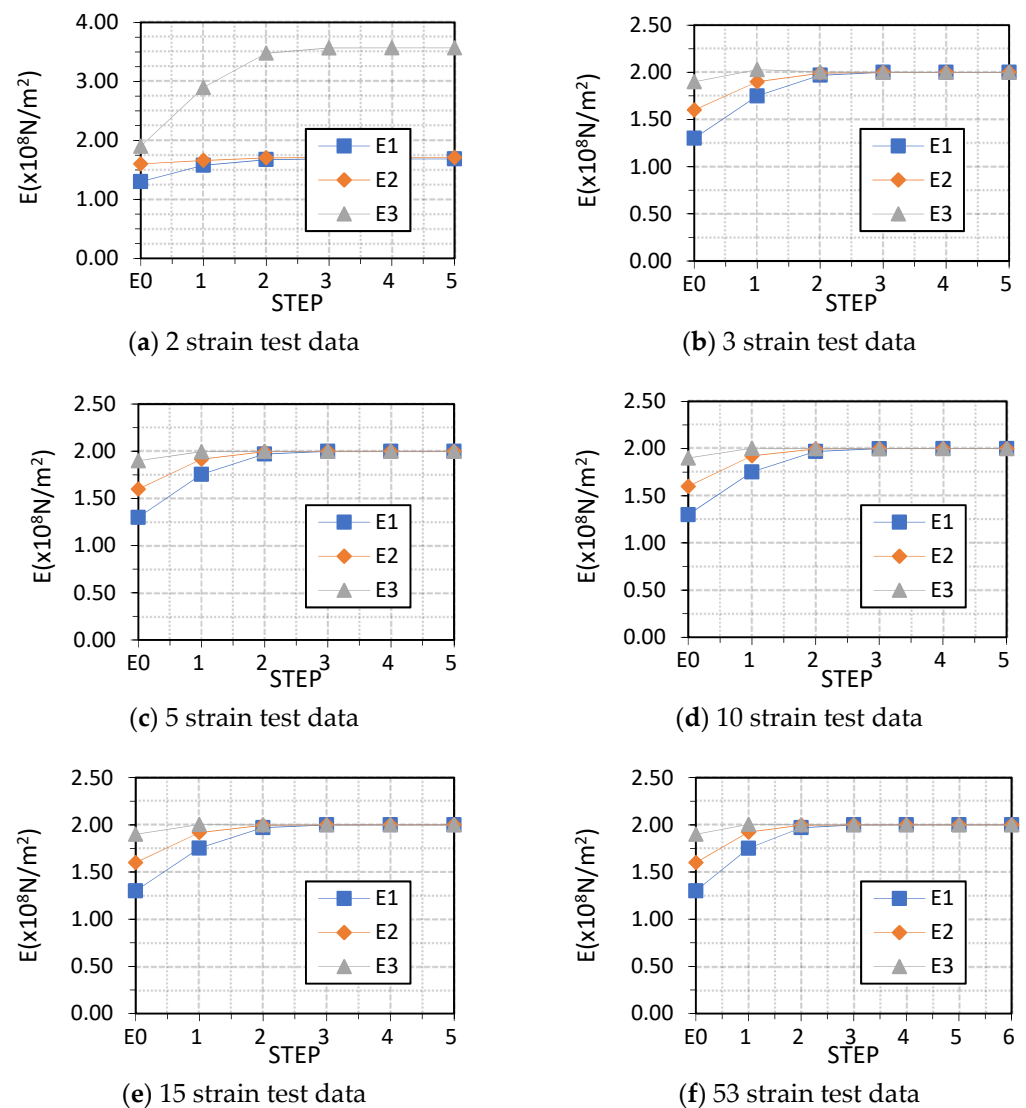


**Figure 3.** Calculation results of different numbers of strain test data.

It can be seen from the above numerical experiment results that when the number of supplementary conditions is less than the number of unknown elastic parameters, the calculation cannot converge to the true elastic moduli value. Thus, the number of supplementary conditions in practical projects is at least greater than or equal to the number of unknown parameters. However, the calculated results are still convergent to the elastic parameters of the model regardless of whether the least three elements or all 53 elements of the strain data are selected as the supplementary conditions. Therefore, in an actual project, it is enough to select a certain number of measured values as additional information, more is not necessarily better. The number of measuring points can be selected according to the actual situation of the site, which not only reduces the construction cost, but also reduces the time cost and improves the operation efficiency.

#### 4.5. Identification of Elastic Parameters with Strain Test Data at Different Locations

We still took  $(1.3, 1.6, 1.9) \times 10^8 \text{ N/m}^2$  as the initial elastic moduli values. When the locations were all scattered at the lower chord (the red part as shown in Figure 4a) and the locations were all concentrated at the support position (the red part as shown in Figure 4b), the iteration process is shown in Tables 6 and 7, respectively.

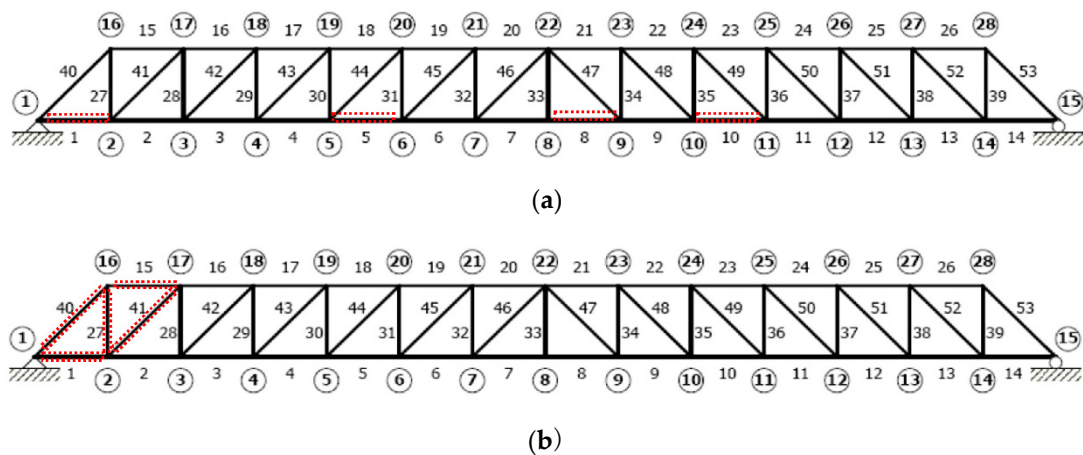


**Figure 4.** (a) Selection of scattered measuring points of the lower chord. (b) Selection of centralized measuring points at the support.

**Table 6.** Calculation results with centralized measuring points of the lower chord.

Number of Iterations	E1	E2	E3	Objective Function
$E_0$	1.30	1.60	1.90	/
0	1.52	2.78	2.43	$3.86 \times 10^{-1}$
1	1.81	2.32	2.09	$1.26 \times 10^{-1}$
2	1.96	2.03	2.02	$2.71 \times 10^{-2}$
3	2.00	2.00	2.00	$1.20 \times 10^{-3}$
4	2.00	2.00	2.00	$5.66 \times 10^{-8}$
5	2.00	2.00	2.00	$1.52 \times 10^{-12}$

**Table 7.** Calculation results with centralized measuring points at the support.

Number of Iterations	E1	E2	E3	Objective Function
$E_0$	1.30	1.60	1.90	/
0	1.64	1.96	2.32	$3.23 \times 10^{-1}$
1	1.91	2.01	2.01	$1.15 \times 10^{-1}$
2	2.00	2.00	2.00	$5.20 \times 10^{-3}$
3	2.00	2.00	2.00	$8.13 \times 10^{-6}$
4	2.00	2.00	2.00	$1.11 \times 10^{-9}$
5	2.00	2.00	2.00	$1.09 \times 10^{-12}$

The above numerical experimental results show that there was little difference in the accuracy of the identification results across different locations of the selected measuring points. The true elastic moduli values could be accurately identified. This is of great significance for practical engineering applications. In practical engineering, according to the actual construction conditions, the time-saving and labor-saving points can be preferentially considered for strain measurement to improve the construction efficiency. Of course, the measuring points with obvious strain change should be selected wherever possible, which is conducive to ensuring the accuracy of the solution.

#### 4.6. Studies on Numerical Stability

In practical engineering, test errors are often caused by other factors such as the accuracy of the instrument or the non-standard test operation. Random errors of +5% and +10% were artificially applied to the strain values of elements 2, 21, 36, and 44 in Table 2, and the calculation results are shown in Table 8. It can be seen from the identification results in Table 8 that after considering the model error, the iteration process is stable and

the solution changes regularly and stably with the change in the error, which proves the good numerical stability of the method in this paper.

**Table 8.** Calculation results under different error conditions.

Step	0%	+5%	+10%
E0	1.3	1.3	1.3
	1.6	1.6	1.6
	1.9	1.9	1.9
1	1.75	1.71	1.67
	1.91	1.84	1.77
	2.01	1.92	1.83
2	1.97	1.88	1.81
	1.99	1.90	1.82
	2.01	1.91	1.82
3	2.00	1.90	1.82
	2.00	1.90	1.82
	2.00	1.90	1.82
4	2.00	1.90	1.82
	2.00	1.90	1.82
	2.00	1.90	1.82
err(%)	0	4.76	9.09
	0	4.76	9.09
	0	4.76	9.09

#### 4.7. Identification under Different Numbers of Unknown Parameters

In practical engineering, the elastic modulus of each region may not be equal, so it should be assumed that the elastic parameters of each measured region are unknown and must be identified. Since the initial value of the initial elastic modulus had no effect on the parameter identification, it was assumed that the initial elastic modulus of all members was  $1.5e8 \text{ N/m}^2$ . The identification results under five unknowns (six simulated test strains were randomly selected), 10 unknowns (11 simulated test strains were randomly selected), 15 unknowns (16 simulated test strains were randomly selected), and the elastic moduli of 53 elements were all unknown (53 test strains are all selected) were studied, respectively. The calculation results of the objective function are shown in Table 9, and the convergence process is shown in Figure 5.

**Table 9.** Convergence process of the objective function under different unknowns.

Number of Iterations	Number of Unknowns			
	5	10	15	53
0	$4.00 \times 10^{-1}$	$7.335 \times 10^{-1}$	1.071	3.536
1	$2.35 \times 10^{-2}$	$4.249 \times 10^{-2}$	$6.250 \times 10^{-1}$	$2.048 \times 10^{-1}$
2	$7.34 \times 10^{-5}$	$1.194 \times 10^{-4}$	$2.968 \times 10^{-3}$	$1.245 \times 10^{-3}$
3	$3.07 \times 10^{-8}$	$6.589 \times 10^{-8}$	$2.278 \times 10^{-3}$	$3.475 \times 10^{-4}$
4	$4.79 \times 10^{-13}$	$6.917 \times 10^{-13}$	$2.078 \times 10^{-5}$	$1.969 \times 10^{-6}$
5			$2.482 \times 10^{-9}$	$1.347 \times 10^{-10}$
6			$2.090 \times 10^{-12}$	$1.277 \times 10^{-12}$

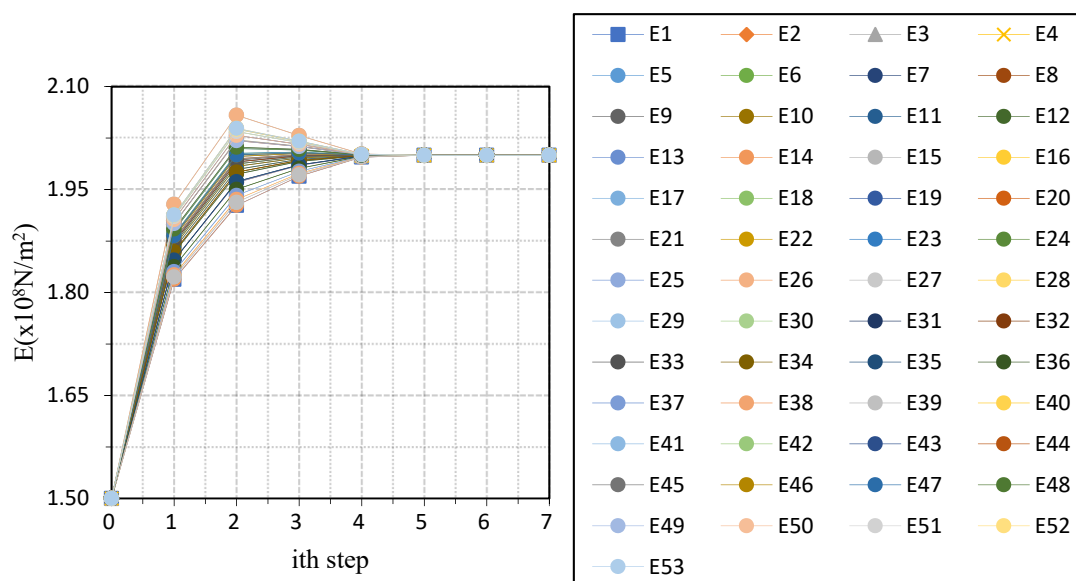


**Figure 5.** Calculation results under 53 unknowns.

When the number of unknowns increased to 53, the calculation results still converged to the true elastic moduli values, which proves the effectiveness of the method when applied to large-scale operations. However, Table 8 shows that when the number of unknowns increased to 15 and 53, more iterations were needed to reach the objective function value than when the number of unknowns was 5 or 10. Thus, when the number increases to a certain extent, the solution process will become longer. In practical engineering, according to the position of the members and their properties in the structure, the members with the same elastic modulus value should be assessed and set as the same unknown parameters as much as possible in combination with prior experience to improve the efficiency of the solution and reduce unnecessary test work.

## 5. Conclusions

In this paper, a mathematical analysis model of elastic modulus identification was constructed, based on strain test data and the improved gradient regularization–finite element method. The numerical analysis showed that the proposed method had very high accuracy and computational efficiency. Finally, the related problems in this paper can be explained and discussed as follows:

(1) The elastic parameter identification method based on the strain test and gradient regularization–finite element method in this paper is available and efficient. However, in practical application, the accuracy of the test data must be ensured. At present, the strain measurement technology for civil structure health monitoring has been very well-developed, the most commonly used being resistance type strain gauges [36], vibrating wire type gauges [37], and fiber optic sensors [38]. At present, the accuracy of the commonly used strain sensors can reach 0.1~0.5  $\mu\epsilon$ . The rapid development of modern testing technology provides a technical guarantee for the proposed method.

(2) In the elastic stage, the proposed method only needs to determine the additional external load and the geometric dimensions of the structure at the moment of the test and has nothing to do with the initial stress of the structure, so it needs less input information and improves the identification accuracy.

(3) In fact, the identification method in this paper is also applicable to the identification of elastic parameters of other structures, but the solution model used in the verse analysis process is different according to the characteristics of various structures.

**Author Contributions:** Conceptualization, Y.Z.; methodology, Y.Z.; software, Y.Z. and A.Z. and H.X.; validation, Y.Z.; formal analysis, Y.Z. and A.Z.; investigation, Y.Z. and A.Z.; data curation, Y.Z. and A.Z.; writing—original draft preparation, Y.Z. and A.Z.; writing—review and editing, Y.Z. and H.Z.; supervision, Y.Z.; project administration, Y.Z.; funding acquisition, Y.Z. All authors have read and agreed to the published version of the manuscript.

**Funding:** This research was funded by [National Natural Science Foundation of China] grant number [50808125].

**Conflicts of Interest:** The authors declare no conflict of interest.

## References

1. Yin, Y.; Wang, S.; Fan, Z.L. Verification of pushover analysis for a long-span steel truss structure. *J. Vibroeng.* **2019**, *21*, 420–430. [[CrossRef](#)]
2. Quaranta, G.; Demartino, C.; Xiao, Y. Experimental dynamic characterization of a new composite glulam-steel truss structure. *J. Build. Eng.* **2019**, *25*, 100773. [[CrossRef](#)]
3. Chang, K.C.; Kim, C.W. Modal-parameter identification and vibration-based damage detection of a damaged steel truss bridge. *Eng. Struct.* **2016**, *122*, 156–173. [[CrossRef](#)]
4. Zhuo, D.B.; Cao, H. Damage identification of bolt connection in steel truss structures by using sound signals. *Struct. Health Monit.* **2022**, *21*, 501–517. [[CrossRef](#)]
5. Luong, H.T.M.; Zabel, V.; Lorenz, W.; Rohrmann, R.G. Vibration-based Model Updating and Identification of Multiple Axial Forces in Truss Structures. *Procedia Eng.* **2017**, *188*, 385–392. [[CrossRef](#)]
6. Luong, H.T.M.; Zabel, V.; Lorenz, W.; Rohrmann, R.G. Non-destructive Assessment of the Axial Stress State in Iron and Steel Truss Structures by Dynamic Measurements. *Procedia Eng.* **2017**, *199*, 3380–3385. [[CrossRef](#)]
7. Liu, K.; Law, S.S.; Zhu, X.Q. System parameter identification from projection of inverse analysis. *J. Sound Vib.* **2017**, *396*, 83–107. [[CrossRef](#)]
8. Cho, S.; Ciles, R.K.; Spencer, B.F. System identification of a historic swing truss bridge using a wireless sensor network employing orientation correction. *Struct. Control. Health Monit.* **2015**, *22*, 255–272. [[CrossRef](#)]
9. Terlaje, A.S.; Trunan, K.Z. Parameter Identification and Damage Detection Using Structural Optimization and Static Response Data. *Adv. Struct. Eng.* **2007**, *10*, 607–621. [[CrossRef](#)]
10. Chakraborty, S.; Islam, A.A. Damage Identification of Steel Trusses from Static Strain Data. *Indian Eng.* **2007**, *83*, 229–232.
11. Song, J.H.; Lee, E.T.; Eun, H.C. Optimal sensor placement through expansion of static strain measurements to static displacements. *Int. J. Distrib. Sens. Netw.* **2021**, *17*, 1550147721991712. [[CrossRef](#)]
12. Wang, H.; Zhu, Q.X.; Li, J.; Mao, J.X.; Hu, S.T.; Zhao, X.X. Identification of moving train loads on railway bridge based on strain monitoring. *Smart Struct. Syst.* **2019**, *23*, 263–278.
13. Meoni, A.; D'Alessandro, A.; Mancinelli, M.; Ubertini, F. A Multichannel Strain Measurement Technique for Nanomodified Smart Cement-Based Sensors in Reinforced Concrete Structures. *Sensors* **2021**, *21*, 5633. [[CrossRef](#)]
14. Matta, F.; Bastianini, F.; Galati, N.; Casadei, P.; Nanni, A. Distributed Strain Measurement in Steel Bridge with Fiber Optic Sensors: Validation through Diagnostic Load Test. *J. Perform. Constr. Facil.* **2008**, *22*, 264–273. [[CrossRef](#)]
15. Goldfeld, Y.; Klar, A. Damage Identification in Reinforced Concrete Beams Using Spatially Distributed Strain Measurements. *J. Struct. Eng.* **2012**, *139*, 1. [[CrossRef](#)]
16. Nick, H.; Aziminejad, A. Vibration-Based Damage Identification in Steel Girder Bridges Using Artificial Neural Network Under Noisy Conditions. *J. Nondestruct. Eval.* **2021**, *40*, 15. [[CrossRef](#)]
17. Weinstein, J.C.; Sanayei, M.; Brenner, B.R. Bridge Damage Identification Using Artificial Neural Networks. *J. Bridge Eng.* **2018**, *23*, 04018084. [[CrossRef](#)]
18. Kuzina, V.; Koshev, A. Modification of the Levenberg–Marquardt Algorithm for Solving Complex Computational Construction Problems. *IOP Conf. Ser. Mater. Sci. Eng.* **2020**, *960*, 032039. [[CrossRef](#)]
19. Izmailov, A.F.; Solodov, M.V.; Uskov, E.I. A globally convergent Levenberg–Marquardt method for equality-constrained optimization. *Comput. Optim. Appl.* **2019**, *72*, 215–239. [[CrossRef](#)]
20. Naseralavi, S.S.; Shojaee, S.; Ahmadi, M. Modified gradient methods hybridized with Tikhonov regularization for damage identification of spatial structure. *Smart Struct. Syst.* **2016**, *18*, 839–864. [[CrossRef](#)]
21. Kadaj, R. The method of detection and localization of configuration defects in geodetic networks by means of Tikhonov regularization. *Rep. Geod. Geoinform.* **2021**, *112*, 19–25. [[CrossRef](#)]
22. Farzaneh, S.; Safari, A.; Parvazi, K. Improving Dam Deformation Analysis Using Least-Squares Variance Component Estimation and Tikhonov Regularization. *J. Surv. Eng.* **2021**, *147*, 04020024. [[CrossRef](#)]
23. Smirnova, A.; Tuncer, N. Inverse problem of groundwater modeling by iteratively regularized Gauss–Newton method with a nonlinear regularization term. *Nonlinear Anal.* **2011**, *74*, 5987–5998. [[CrossRef](#)]
24. Artar, M.; Daloglu, A. Damage detection in simulated space frames using genetic algorithms. *Sigma J. Eng. Nat. Sci.* **2015**, *33*, 166–187.

25. Tang, L.M.; Zhang, W.F.; Liu, Y.X. Gradient-Regularization Method to Solve the Inverse Problems of Differential Equation. *Chin. J. Comput. Mech.* **1991**, *8*, 123–129.
26. Liu, Y.X.; Wang, D.G.; Zhang, J.L.; Li, J.S.; Lu, Z.G.; Yu, Y.J. Identification of material parameters with gradient regularization method. *Chin. J. Comput. Mech.* **2000**, *17*, 69–75.
27. Giraud, J.; Lindsay, M.; Ogarko, V.; Jessell, M.; Martin, R.; Pakyuz-Charrier, E. Integration of geoscientific uncertainty into geophysical inversion by means of local gradient regularization. *Solid Earth* **2019**, *10*, 193–210. [[CrossRef](#)]
28. Zhang, Y.X.; Li, G.Q.; Zhang, J.L. Structural elastic modulus identification based on finite element regularization method. *Eng. Mech.* **2007**, *10*, 6–10.
29. Cui, K.; Li, X.S.; Li, B.Y.; Yang, G.W. Global convergence gradient regularization algorithm for solving nonlinear inverse problems. *Chin. J. Comput. Mech.* **2005**, *4*, 415–419.
30. Reichel, L.; Rodriguez, G. Old and new parameter choice rules for discrete ill-posed problems. *Numer. Algorithms* **2013**, *63*, 65–87. [[CrossRef](#)]
31. Hua, X.G.; Ni, Y.Q.; Ko, J.M. Adaptive regularization parameter optimization in output-error-based finite element model updating. *Mech. Syst. Signal Process.* **2009**, *23*, 563–579. [[CrossRef](#)]
32. Hansen, P.C.; Leary, D.P. The Use of the L-Curve in the Regularization of Discrete Ill-Posed Problems. *SIAM J. Sci. Comput.* **2006**, *14*, 1487–1503. [[CrossRef](#)]
33. Bucataru, M.; Cimpean, I.; Marin, L. A gradient-based regularization algorithm for the Cauchy problem in steady-state anisotropic heat conduction. *Comput. Math. Appl.* **2022**, *119*, 220–240. [[CrossRef](#)]
34. Morozov, V.A. *Methods for Solving Incorrectly Posed Problems*; Springer: New York, NY, USA, 1984.
35. Gao, Y. *Structural Health Monitoring Strategies for Smart Sensor Networks*; Newmark Structural Engineering Laboratory (NSEL) Report Series, No. 13; University of Illinois: Urbana, IL, USA, 2008; Available online: <http://hdl.handle.net/2142/8802> (accessed on 10 October 2021).
36. Copertaro, E. Assessment of resistive strain gauges measurement performances in experimental modal analysis and their application to the diagnostics of abrasive waterjet cutting machinery. *Measurement* **2022**, *188*, 110626. [[CrossRef](#)]
37. Peng, L.; Jing, G.Q.; Wang, Y.X.; Miao, N. Research on Calibration Model of Bridge Health Monitoring Based on Vibrating Wire Strain Sensor. *Earth Environ. Sci.* **2021**, *692*, 042099. [[CrossRef](#)]
38. Yan, M.; Tan, X.; Mahjoubi, S.; Bao, Y. Strain transfer effect on measurements with distributed fiber optic sensors. *Autom. Constr.* **2022**, *139*, 104262. [[CrossRef](#)]